



HHS PUBLIC ACCESS

Author manuscript

ACS Infect Dis. Author manuscript; available in PMC 2017 January 08.

Published in final edited form as:

ACS Infect Dis. 2016 January 8; 2(1): 82–92. doi:10.1021/acsinfecdis.5b00108.

Using Computational Modeling To Optimize the Design of Antibodies That Trap Viruses in Mucus

Timothy Wessler^{†,||}, Alex Chen^{†, ||}, Scott A. McKinley[§], Richard Cone[⊗], Gregory Forest^{†,⊥,*}, and Samuel K. Lai^{‡,⊥,#,*}

[†]Departments of Mathematics and Applied Physical Science, University of North Carolina—Chapel Hill, Chapel Hill, North Carolina 27599, United States

[§]Mathematics Department, Tulane University, New Orleans, Louisiana 70118, United States

[⊗]Department of Biophysics, Johns Hopkins University, Baltimore, Maryland 21218, United States

[‡]Division of Molecular Pharmaceutics, Eshelman School of Pharmacy, University of North Carolina—Chapel Hill, Chapel Hill, North Carolina 27599, United States

[⊥]UNC/NCSU Joint Department of Biomedical Engineering, University of North Carolina—Chapel Hill, Chapel Hill, North Carolina 27599, United States

[#]Department of Microbiology & Immunology, University of North Carolina—Chapel Hill, Chapel Hill, North Carolina 27599, United States

Abstract

Immunoglobulin G (IgG) antibodies that trap viruses in cervicovaginal mucus (CVM) via adhesive interactions between IgG-Fc and mucins have recently emerged as a promising strategy to block vaginally transmitted infections. The array of IgG bound to a virus particle appears to trap the virus by making multiple weak affinity bonds to the fibrous mucins that form the mucus gel. However, the antibody characteristics that maximize virus trapping and minimize viral infectivity remain poorly understood. Toward this goal, we developed a mathematical model that takes into account physiologically relevant spatial dimensions and time scales, binding, and unbinding rates between IgG and virions and between IgG and mucins, as well as the respective diffusivities of virions and IgG in semen and CVM. We then systematically explored the IgG–antigen and IgG–mucin binding and unbinding rates that minimize the flux of infectious HIV arriving at the vaginal epithelium. Surprisingly, contrary to common intuition that infectivity would drop monotonically with increasing affinities between IgG and HIV, and between IgG and mucins, our model suggests

*Corresponding Authors. (S.K.L.) Mail: Division of Molecular Pharmaceutics, Eshelman School of Pharmacy, University of North Carolina—Chapel Hill, Marsico Hall 4213, 125 Mason Farm Road, Campus Box 7362, Chapel Hill, NC 27599, USA. Phone: (919) 966-3024. lai@unc.edu. (M.G.F.) Phone: (919) 962-9606 forest@unc.edu.

Present Address, (A.C.) Risk Analytics Laboratory, GE Global Research Center, K1-4A54A, 1 Research Circle, Niskayuna, NY 12309, USA.

^{||}T.W. and A.C. contributed equally.

ASSOCIATED CONTENT

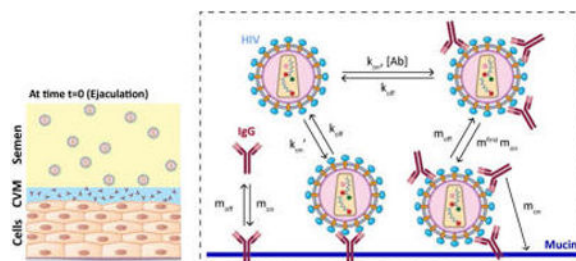
Supporting Information

The Supporting Information is available free of charge on the ACS Publications website at DOI: [10.1021/acsinfecdis.5b00108](https://doi.org/10.1021/acsinfecdis.5b00108).

Supporting methods (derivation of probability distributions for the amount of time virions spend interacting with mucins vs freely diffusing, and theoretical estimates of IgG–mucin bond rates and times) and Figures S1–S4 (PDF)

The authors declare no competing financial interest.

maximal trapping of HIV and minimal flux of HIV to the epithelium are achieved with IgG molecules that exhibit (i) rapid antigen binding (high k_{on}) rather than very slow unbinding (low k_{off}), that is, high-affinity binding to the virion, and (ii) relatively weak affinity with mucins. These results provide important insights into the design of more potent “mucotrapping” IgG for enhanced protection against vaginally transmitted infections. The model is adaptable to other pathogens, mucosal barriers, geometries, and kinetic and diffusional effects, providing a tool for hypothesis testing and producing quantitative insights into the dynamics of immune-mediated protection.



Keywords

HIV; cervicovaginal mucus; mucin; IgG; mucosal immunity; sexually transmitted infections

Antibodies (Abs) produced by our immune system are found in abundant quantities in both blood and mucosal secretions and serve as key molecules that help regulate numerous complex defense mechanisms against foreign pathogens.¹ For example, Abs can directly block contact between viruses and target cells, a process known as neutralization.² Abs can also facilitate other protective functions, such as ingestion and destruction of the pathogens (opsonization) or infected cells (antibody-dependent cellular cytotoxicity, or ADCC) by specialized immune cells, as well as activation of a cascade of enzymes that lead to direct lysis of the pathogen membrane (complement).³ These various protective mechanisms most certainly contribute to the robust protection observed with topically delivered Abs against mucosally transmitted infections in a multitude of animal studies.⁴

In the female reproductive tract, immunoglobulin G (IgG) is the predominant Ab secreted into cervicovaginal mucus (CVM) coating the vaginal epithelium,⁵ yet its role in protection against vaginal infections is not yet well understood. CVM is composed primarily of a heterogeneous mesh network of mucin fibers with low viscosity fluid-filled pores, most of which are larger than the majority of viruses.⁶ Indeed, HIV virions are capable of diffusing nearly unimpeded through the mucus gel.⁷ Noting the abundance of Abs produced and secreted by the immune system into mucus secretions, we hypothesized that virus-specific IgG may work in tandem with the mucin mesh to prevent infections. We recently showed that IgG can indeed trap viruses in CVM, thereby facilitating an additional and highly potent mechanism of immune protection.^{5c} Interestingly, the diffusivity of IgG in mucus is only slowed ~10–20% compared to in buffer;⁸ hence, individual IgG molecules must make only weak and transient bonds with mucins and thus were previously thought incapable of effectively trapping viruses in mucus gels. Nevertheless, as IgG accumulates on the virus surface, the array of virion-bound IgG can collectively form *multiple* weak Ab–mucin bonds

between the virion and CVM, thereby generating sufficient avidity to slow or even immobilize individual virions in mucus akin to multiple weak links formed by a Velcro patch. Trapping viruses in mucus not only reduces the flux of virus reaching target cells in the vaginal epithelium, but trapped viruses are also quickly eliminated along with natural mucus clearance mechanisms, as evident by protection against vaginal herpes transmission using a non-neutralizing monoclonal IgG.^{5c}

Many viruses, including HIV, can rapidly diffuse through mucus gels under physiological conditions, limiting the window of opportunity for Abs to accumulate on the virus surface before the virus reaches and infects the underlying vaginal epithelium.⁹ The extent to which IgG can hinder the diffusion of viruses in mucus, and consequently the potency of protection based on IgG-mediated trapping of viruses, is thus critically dependent on whether virus-specific IgG, topically delivered or elicited by vaccine or prior infection, can accumulate rapidly enough on a virion and impart sufficient binding avidity between the virion and mucus to trap the virus before it can reach the underlying cells. We are interested in developing potent “muco-trapping” IgG (i.e., that enables effective trapping with fewer virion-bound IgG) not only because this would (i) reduce the dose of IgG needed for passive immunization of the vagina but also because this would (ii) likely improve protection against viruses, such as HIV, that have only a small number of antigens on their surface.

Our aim quickly posed a conundrum: although fewer virus-bound IgGs would be needed to trap a virus if each bound IgG binds more tightly to mucins, high IgG affinity to mucins would reduce or even prevent the diffusive mobility of IgG in the mucus gel. Because the Smoluchowski encounter rate between two diffusive species is proportional to the sum of their diffusivities, mucin-associated IgG would therefore have markedly reduced encounters with virions and, by definition, exhibit lower rates of binding to viral antigens. The IgG–mucin and IgG–antigen affinities and actual binding/unbinding rates that maximize viral trapping and protection will depend on specific characteristics of the target virus, such as its diffusivity in mucus and surface antigen density.

Because an empirical, experimental determination of these numerous parameters and their relative contributions to trapping and protection remains exceedingly challenging, we turned to mathematical modeling to better understand the subtle interplay between the various kinetic and diffusive processes among IgG, virions, and CVM during vaginal transmission of sexually transmitted viruses. Specifically, we consider CVM containing a specific concentration of antigen-specific IgGs that possess tunable binding and unbinding kinetics to mucins in CVM subjected to introduction of virus-laden semen (Figure 1). With a mathematical model, starting from the moment of viral deposition in the female reproductive tract, we can model the subsequent codiffusion of virions and IgG as well as the binding and unbinding kinetics among IgG molecules, viruses, and mucins and freely explore the vast parameter space in the context of physiologically relevant spatial dimensions and time scales. As a proof-of-concept, we focused on HIV, given the great need for alternative strategies to prevent vaginal HIV transmission; indeed, passive immunization has recently garnered attention as a promising approach for HIV prophylaxis.¹⁰ In turn, the model allows us to explore whether, and the extent to which, tuning IgG–mucin affinity can facilitate improved protection against vaginal HIV infection. In doing so, we report that the model

suggests a “sweet spot” in the characteristics of IgG that maximize trapping and minimize infectious flux of HIV to the vaginal epithelium.

RESULTS

Incorporating Mucin-Binding Kinetics into Previous Models for HIV Penetration of Ab-Laden CVM

We have previously modeled the diffusion of HIV through CVM by combining a stochastic/deterministic hybrid model for the one-dimensional Brownian movement of individual HIV virions together with a continuum model that describes the average local concentration of broadly neutralizing monoclonal IgG in CVM.¹¹ That model allowed us to show that a multitude of weak bonds between virion-bound IgG and mucins alone, defined by the ratios of IgG diffusion in mucus versus buffer (α) in the range of 0.8–0.9, is sufficient to immobilize the vast majority of HIV near the semen/CVM interface. Nevertheless, to further explore the IgG trapping potency across the full range of IgG–mucin affinity, it was necessary to incorporate additional complexity into the model. First, when modeling IgG that binds more tightly to mucins, we made the assumption that the probability of a successful bond between an IgG molecule and the corresponding viral antigen is directly proportional to the overall collision frequencies between the two bodies, which can be described by the classical Smoluchowski principle.¹² Because an IgG bound to mucins will possess a far reduced range of motion relative to that of a free, unbound IgG molecule, the bound IgG should possess a reduced k_{on} rate, denoted k_{on}' , proportional to the reduction in collision frequency with viral antigen, which in turn can be approximated by the ratios of the diffusivity of IgG versus mucins in CVM. Although the diffusivity of individual mucins in CVM remains unknown, we have previously shown that CVM is composed of heavily bundled mucins that likely reflect an exceedingly limited range of motion for individual mucins.⁶ We thus made a very conservative estimate that an IgG bound to mucin will possess a 30-fold reduced k_{on} rate compared to individual free IgG (i.e., $k_{\text{on}}' = k_{\text{on}}/30$), which roughly equates to assuming the range of motion of mucins to match that for individual HIV virions. Although obviously an overconservative assumption, further reduction in k_{on}' does not meaningfully affect estimates generated by our model (Figure S4).

A second important detail we incorporated into our model is the kinetics of IgG binding to and unbinding from mucins, which we termed m_{on} and m_{off} , respectively. Experimentally, m_{on} and m_{off} appear to be extremely transient and difficult to measure individually⁸ (see also the Supporting Information). Instead, IgG–mucin affinity is inherently reflected by the diffusion coefficients of IgG in CVM versus in buffer, which we denote α . α reflects the fraction of bound versus unbound IgG at any moment in time and is equivalent to the ratio $m_{\text{off}}/(m_{\text{off}} + [M]m_{\text{on}})$ at steady state. Assuming IgG binding to its antigen does not increase its affinity to mucins, the rates with which individual IgG can bind to mucins must be far faster than the rate of virion-associated IgG binding to mucins. We thus introduced a correction factor of ~ 30 for the mucin-association kinetics for virion-bound IgG, which is equivalent to the difference in diffusivities of HIV versus IgG in CVM. This correction was necessary to ensure we do not overestimate the trapping potency of viruses.

As a first step toward understanding how IgG–mucin affinity can affect trapping potency, we modeled the probability and duration of HIV–IgG complexes associating with mucins in CVM containing 1 $\mu\text{g/mL}$ NIH45-46 with varying IgG–mucin affinity. Naturally, HIV with surface IgG possessing no affinity to mucins, defined by $\alpha = 1$, never binds to mucins, and the HIV–IgG complex undergoes free diffusion for the entire duration (Figure 2A). When IgG–mucin affinity is slightly increased such that individual IgGs associate with mucins ~5 and 10% of the time (i.e., $\alpha = 0.95$ and 0.9 , respectively), the fraction of time an HIV–IgG complex spends freely diffusing in mucus begins to decrease, with a corresponding increase in the fraction of time spent associated with mucins (Figure 2B,C). Interestingly, the fraction of time the HIV–IgG complex associates with mucins appears to peak between $\alpha = 0.1$ and 0.25 (Figure 2D–F). This is attributed to the facts that (i) increased IgG–mucin affinity markedly reduces the fraction of NIH45-46 that can freely diffuse and readily bind to HIV, including IgG that diffuses from CVM into the semen layer and binds to HIV virions before they enter the CVM layer (Figure S2); and (ii) mucin-associated IgG captures HIV with far lower efficiency (i.e., reduced k_{on}' vs k_{on}). These two factors together increase the number of HIV virions with no bound IgG. With further increases of mucin affinity to $\alpha = 0.01$, the amount of HIV free of bound IgG dominates relative to HIV–IgG complexes, and most HIV again undergoes Brownian motion in CVM (Figure 2G).

Influence of IgG–Mucin Affinity on Maximizing Trapping Potency and Vaginal Protection

We next quantified how the probability of HIV–mucin association affects the fraction of HIV that can penetrate CVM and reach the underlying vaginal epithelium and the corresponding reduction in infectivity based on the decrease in HIV–Env free of bound IgG on those virions.⁹ In good agreement with the estimate of the fraction of time spent associated with mucins, the maximum reduction in HIV flux reaching the vaginal epithelium peaks at IgG–mucin affinities corresponding to $\alpha = 0.25$ (Figure 3A). At 5 and 10 $\mu\text{g/mL}$ NIH45-46 initially present in CVM and an IgG–mucin affinity equivalent to $\alpha = 0.25$, only ~3 and ~0.3% of the HIV viral load in semen, respectively, are predicted to reach the vaginal epithelium over the first 2 h post-ejaculation, equating to 10–100-fold reduced flux compared to the estimated ~30% of HIV load over the same duration in the absence of IgG–mucin affinity (Figure 3A). Under this scenario, each HIV virion on average possesses ~2 bound IgGs (Figure 3B), and the overall infectivity is reduced by 86–94% (i.e., ~7–16-fold) compared to IgG without affinity to mucins (Figure 3C,D). Note that the reduction in infectivity is less than the reduction in the flux of HIV viruses because NIH45-46 without affinity to mucins can still neutralize the virus.

When IgG–mucin affinity is further increased (i.e., lower α), the fraction of HIV reaching the vaginal epithelium begins to increase. Furthermore, there are also substantially fewer IgGs bound to HIV–Env on virions that reach the vaginal epithelium. Indeed, when α drops below 0.1, on average <1 IgG molecule is bound to each virion over the entire population of HIV virions, which implies that there must be HIV virions without any bound IgG (Figure 3B). As a result, the infectivity of HIV may actually be greater for hypothetical NIH45-46 that can bind tightly to mucins than if NIH45-46 possessed no mucin affinity at all (Figure 3C,D).

To begin to understand how to engineer more potent HIV-trapping IgG, we evaluated the relative impact of the rate of IgG binding to the virus surface compared to IgG–mucin affinity. The rate of IgG binding to HIV is the product of both the local IgG concentration and k_{on} , the binding kinetic constant: a doubling of IgG k_{on} has the same impact on IgG binding to HIV as doubling the IgG concentration. The reduction of HIV flux arriving at the vaginal epithelium and the reduction in mean number of NIH45-46-free Env proteins on HIV that reached the vaginal epithelium were sensitive to both IgG–antigen binding rate and IgG–mucin affinity (Figure 4). When IgG–mucin affinity was increased, the amount of initial NIH45-46 in CVM needed to reduce the flux of viruses arriving at the vaginal epithelium by 50% decreased from 5 to 50 $\mu\text{g/mL}$ for $\alpha = 0.8$ – 0.9 (this IgG–mucin affinity is within the range of what was previously measured for IgG in CVM) to <1 $\mu\text{g/mL}$ when $\alpha = 0.25$ (Figure 4A). Similarly, the amount of NIH45-46 needed to reduce the mean number of NIH45-46-free Env proteins on HIV by 80% decreased from 26 $\mu\text{g/mL}$ for $\alpha = 0.8$ to 3 $\mu\text{g/mL}$ for $\alpha = 0.25$ (Figure 4D). Overall, the amount of NIH45-46 needed to reduce infectivity by 90% decreased from 7 $\mu\text{g/mL}$ when $\alpha = 1$ to 2 $\mu\text{g/mL}$ when $\alpha = 0.25$ (Figure 4C).

Influence of IgG–Antigen Binding Affinity on Maximizing Trapping Potency and Vaginal Protection

A longstanding assumption for neutralizing IgG against HIV and other viruses is that higher binding affinity between IgG and viral antigen facilitates more potent protection. However, it is important to note that high-affinity IgGs are typically identified and selected on the basis of neutralization assays in the absence of mucus coatings and with some incubation time between virus and IgG prior to exposure of the virus to target cells. Thus, we sought to quantitatively evaluate whether a high antigen–IgG affinity that typically maximizes neutralization potency in vitro would also be maximally protective against mucosal HIV transmission in our model.

Interestingly, we found that the antigen-unbinding rate k_{off} generally possessed only a very minor effect on increasing the fraction of HIV load that is trapped in mucus or facilitating more effective protection, especially when the IgG concentration or the k_{on} rate is low (Figure 5A). For example, at 1 $\mu\text{g/mL}$ of IgG with k_{on} of $1.5 \times 10^4 \text{ M}^{-1} \text{ s}^{-1}$ ($k_{\text{on}}[\text{Ab}] = 10^{-4} \text{ s}^{-1}$), improvements of k_{off} from 10^{-3} s^{-1} to 10^{-4} s^{-1} reduced the HIV flux arriving the vaginal epithelium by only 1.6%, and a further improvement from 10^{-4} s^{-1} to 10^{-5} s^{-1} essentially resulted in no appreciable difference in reduction of flux (Figure 5A). This is similarly reflected by the minimal change in the infectivity of the viruses relative to IgG with no mucin affinity from 100% with $k_{\text{off}} = 10^{-3} \text{ s}^{-1}$ to 96% with $k_{\text{off}} = 10^{-4} \text{ s}^{-1}$ to finally 92% with $k_{\text{off}} = 10^{-5} \text{ s}^{-1}$ (Figure 5C,D). The lack of impact by k_{off} is directly attributed to the exceedingly limited number of IgG molecules that can accumulate on the surface of HIV either when IgG is present at low to modest concentrations or when IgG possesses inadequate binding kinetics (Figure 5B); slower unbinding kinetics simply cannot enhance HIV trapping in mucus or neutralization when few or no IgGs are bound to HIV in the first place.

In contrast to k_{off} , the IgG–antigen binding rate k_{on} plays a far more critical role in effective mucosal protection. Because the rate of IgG accumulation on the virion surface is the product of the IgG concentration and k_{on} , increasing IgG k_{on} by definition would have the same magnitude of impact as increasing IgG concentration. In other words, a 10-fold faster k_{on} would reduce the fraction of HIV reaching the vaginal epithelium and overall infectivity to the same extent as increasing the total HIV-binding IgG in CVM by 10-fold (Figure 5A), because both would result in the same increase in the number of IgG bound to HIV before the virions can reach the vaginal epithelium. Our current finding on the relative importance of k_{on} versus k_{off} is consistent with an earlier investigation that simply evaluated the kinetics of neutralization, which did not take into account IgG–mucin interactions.¹¹ Incorporating IgG–mucin affinity appears to amplify the difference, likely because rapidly binding IgG can protect by either trapping or neutralization, and viruses slowed by IgG–mucin interactions will also be more completely neutralized prior to reaching target cells underlying the vaginal epithelium.

DISCUSSION

A hallmark of HIV is its exceptionally high mutation rate, which enables the virus to readily escape antibodies generated by the immune system and prevents the host from mounting a protective immune response. Comprehensive studies of elite controllers—the rare individuals who can maintain undetectable viral load without antiretroviral therapy—led to the discovery and cloning of monoclonal antibodies that can broadly neutralize the vast majority of HIV strains. These broadly neutralizing antibodies (bnAbs) were thought to provide a template for the development of an HIV vaccine. Unfortunately, HIV vaccines, including those that can block vaginal transmission of HIV, remain elusive to date, for at least two reasons. First, bnAbs are typically highly somatically mutated, and vaccines may not be able to elicit the extent of somatic hypermutation needed in most individuals to generate the desirable bnAbs. Second, many HIV vaccine candidates are based on DNA or subunit proteins rather than attenuated virus; the durability of antibody response from subunit vaccines is generally shorter than that of vaccines based on attenuated virus, and the level of antibody titers induced in the vagina may be inadequate to block vaginal HIV transmission.

To overcome these challenges, a recently emerged strategy is to passively immunize the vagina via sustained delivery of bnAbs.^{10b, 13} By dosing the bnAbs directly into the vagina, this strategy not only bypasses the limitations of somatic hypermutation but also ensures protective levels of bnAbs are present in the vagina to block HIV transmission. Despite these important advantages, a critical shortcoming for passive immunization is the relatively high cost of maintaining protective levels of antibody in the body compared to vaccination. Much effort has been spent on reducing the costs of antibody production, such as the production of antibodies in plants,¹⁴ as well as cheaper and more efficient methods of purifying antibodies.¹⁵ Here, we introduce a novel and completely distinct approach—based on tuning IgG–mucin interactions—that could markedly reduce the dose of bnAbs needed to block vaginal HIV transmission. The majority of bnAbs against HIV appear to possess k_{on} in the range of 10^4 M s^{-1} , which we previously estimated may require concentrations in excess of 5–10 $\mu\text{g/mL}$ to facilitate effective protection. Although we predict enhanced

vaginal protection can be accomplished with both increasing k_{on} and optimizing IgG–mucin affinity, bnAbs generally bind to a very unique epitope on HIV-Env that makes it unlikely that k_{on} can be substantially improved without compromising binding affinity (i.e., resulting in higher k_{off}). In contrast, simply by tuning the interactions between IgG–Fc and mucins, we can potentially reduce the required dose of bnAb for effective protection by 3.5-fold or more without jeopardizing the broad antigen coverage of bnAb. Optimizing IgG–Fc interactions with mucins thus offers a promising strategy to markedly reduce the costs for effective passive immunization of the vagina. The convergence of these various approaches may synergistically drive down costs and make passive immune protection against HIV cost-effective even in resource-poor settings.

Surprisingly, our model suggests that high-affinity IgG–mucin interactions are unlikely to enhance protection. Instead, the ideal IgG–mucin affinity that maximizes protection in our model ($\alpha \sim 0.25$) is comparable to the mucin affinity previously measured for IgM molecules.⁸ It is also worth noting that IgM, due to its pentameric structure, has 10 Fab arms compared to 2 Fab arms for each IgG and hence can bind to its antigenic target and accumulate on the surface of virions with exceptional speed even if each Fab possesses relatively poor affinity compared to a fully affinity-matured IgG. Thus, an IgM molecule appears to simultaneously satisfy both of the design requirements we have identified in this study—rapid k_{on} and modest mucin affinity. Indeed, we recently found that IgM that binds HIV-sized nanoparticles exhibited greater mucotrapping potency than corresponding IgG (Henry et al., submitted for publication). IgM is the first antibody isotype produced by our immune system and appears early in the course of an infection. Virus-specific IgM also usually reappears upon re-infection. Although speculative, our study raises the hypothesis that an evolved effector function of IgM may be to quickly begin purging a new pathogen from mucosal surfaces that likely represent the initial site of infection early in the course of infection, and thereby minimize the viral titers that can enter the systemic circulation.

As discussed above, it is unlikely that we can markedly improve the k_{on} for bnAbs without potentially compromising their broad antigenic coverage. An alternative method to enhance the overall rate of IgG accumulating on the viral surface at mucosal secretions is to include IgG targeting other viral epitopes, including potentially non-neutralizing epitopes, because trapping virions in mucus requires only binding and not necessarily neutralizing IgG. It is important to note that the immune system typically generates a polyclonal Ab response against diverse epitopes, rather than solely a neutralizing Ab response against a single viral epitope. Indeed, many of the naturally produced IgG against HIV found in HIV patients associate with either the lipid membrane of HIV virions, or other parts of the gp120 site on the Env spike not directly involved in HIV infection of immune cells.¹⁶ Likewise, virtually all of the IgGs detected in the moderately successful RV144 trial were non-neutralizing.¹⁷ Such a polyclonal response would likely result in a substantially faster rate of Ab accumulation than with an individual monoclonal IgG. Thus, codelivery of multiple IgGs to enhance passive immune protection of the vagina, or inclusion of multiple immunogens (including non-neutralizing epitopes) in vaccine formulations, would both harness the same strategy our immune system has evolved to fend off foreign pathogens.

Although often under-appreciated, CVM represents the first line of defense against sexually transmitted infections in the female reproductive tract. In addition to minimizing trauma to the vaginal epithelium upon coital stirring, the presence of the CVM layer also prevents virions in semen from immediately contacting the vaginal epithelium upon ejaculation and directly reduces the virion flux and total viral load in semen that can reach target cells over time. Reinforcing the CVM barrier against sexually transmitted viral infections using virus-specific Abs that trap viruses in mucus is likely an important mechanism of the vaginal mucosal defense, but one that continues to be largely under-appreciated and under-explored. We expect that the combination of quantitative, predictive models with experimental validation will enable development of improved passive immunization as well as vaccination methods that harness the mucus barrier to reinforce mucosal defense against HIV and other sexually transmitted infections.

MATERIALS AND METHODS

Model Parameters for Vaginal Transmission of Cell-free HIV

In the female reproductive tract, mucus flows into the vagina from the cervical os, spreads over the vaginal epithelium, and is eventually cleared through the introitus. In this process, the thickness of the CVM layer likely varies within the vagina, with the thickest layer likely to be at the cervical os and vagina fornices, the thinnest near the introitus, and possibly substantial variations throughout. In the absence of experimental measurements of the thickness of the mucus layer coating the human vagina, we made the assumption that CVM approximately evenly covers the entire vaginal epithelial surface, due to spreading by repeated coital motion. We estimated the CVM layer thickness by dividing the volume of mucus ($\sim 750 \mu\text{L}$; range typically between $500 \mu\text{L}$ and 2 mL) with the approximate surface area of the vaginal lumen (145 cm^2 ; ¹⁸ Table 1), which results in a thickness of roughly $L = 50 \mu\text{m}$. Our estimate of approximate mucus volume is based on the volume that may be collected by repeated use of a menstrual collection device, the Inseam Softcup, which we have utilized in prior studies.^{5c,6,7a,b,19} Although the Softcup is intended to be placed over the cervical os during menses, in our studies, donors typically insert the Softcup for only 5–10 s. Due to the limited duration of insertion, the mucus we collect reflects predominantly mucus overlaying the vaginal surface that was gathered on the SoftCup during the insertion/extraction process, rather than mucus that flowed out of the cervical os and pooled onto the cup over many hours. This procedure allows us to obtain substantial volumes of mucus that contains the same microbial communities and densities as sampling by vaginal swabs.^{7b}

Similar to previous studies,^{9,11,20} we modeled the diffusion of HIV ($D_{\text{HIV}} \sim 1.27 \mu\text{m}^2/\text{s}$ ¹¹) from a virion-rich layer of semen (8.4×10^5 virions, the average viremia in semen of acutely infected males^{9,21} in an ejaculate volume of $\sim 3.0 \text{ mL}$ ²²) uniformly deposited on the luminal surface of the CVM layer. This results in a thickness of $d = 200 \mu\text{m}$ for the semen layer. Neutralizing Abs ($D_{\text{Ab}} \sim 40 \mu\text{m}^2/\text{s}$ ¹¹) accumulate on HIV virions at rates depending on Ab–antigen affinity, the number of available antigen sites on the virus surface, the local Ab concentration, and the diffusivity of the Abs in CVM. For a model monoclonal broadly neutralizing Ab against HIV, we focused on NIH45-46, which binds to the CD4 binding site of gp120 and whose binding affinities were previously described.²³ The number of Env

spikes N_* on individual HIV virions is variable and was estimated to follow a negative binomial distribution with $N_* = 14 \pm 7$ (range 4–35) based on cryoelectron microscopy of HIV virions.²⁴

Ab Binding to HIV Env Spikes

We assume each Env spike can bind up to three Abs without significant steric hindrance; thus, individual Abs at concentration $u(z,t)$ can bind and unbind independently with rates k_{on} and k_{off} , and overall binding/unbinding rates depend on the number of unoccupied binding sites $3N_* - n$, where n is the number of bound Ab. However, because the diffusivity for a mucin-bound Ab $u_b(z,t)$ is reduced compared to free individual Ab, the Smoluchowski encounter rate, which describes the collision rate of two populations of spherical particles diffusing freely in three dimensions, implies that the binding rate for a mucin-bound Ab (k'_{on}) to its antigen should be reduced proportionally to the difference in diffusivities of the Ab (D_{Ab}) and the virus (D_v); hence, $k'_{\text{on}} = (D_v / (D_{\text{Ab}} + D_v)) k_{\text{on}} \approx (1/30) k_{\text{on}}$. The Ab–virion binding rate equations can be summarized as

$$(\text{Ab}) + (\text{Ab})^n Z(t) \xrightleftharpoons[(n+1)k_{\text{off}}]{(3N_*-n)(k_{\text{on}}^f u_f(Z(t),t) + k_{\text{on}}^b u_b(Z(t),t))} (\text{Ab})^{n+1} Z(t) \quad (1)$$

where (Ab) is an unbound Ab, $(\text{Ab})^n Z(t)$ denotes a virion at $Z(t)$ with n bound Ab, and superscript/subscript f and b denote free and bound terms, respectively. Individual Abs also bind and unbind to mucins at rates $m_{\text{on}}[\text{M}]$ and m_{off} , where $[\text{M}]$ is the effective concentration of Ab binding sites in the mucin network. In addition, virion-bound Abs may associate with mucins, effectively immobilizing the entire Ab–virion complex for the duration of the interaction.

HIV Diffusion through CVM

We developed two different methods to simulate HIV penetration across the vaginal mucus layer. In the first method, a stochastic particle simulation was used for virion diffusion, virion–Ab binding, and Ab–mucin interactions. Because the number of Abs is much larger than the number of virions, we utilized a diffusion partial differential equation (PDE) for the Ab concentration. Virion diffusion for a particle Z is given by the stochastic differential

equation (SDE) $dZ = (2D)^{1/2} dW$, where W is Brownian motion and $D = \begin{cases} D_{\text{HIV}} & \text{free} \\ 0, & \text{bound} \end{cases}$, where “free” indicates that all virion-bound Abs are free from mucin and “bound” indicates that at least one virion-bound Ab is associated with mucin. We assume Brownian diffusion of virions based on our previous findings that HIV and other viruses and nanoparticles can diffuse nearly unobstructed in CVM.^{5c,7a,b,19} Importantly, although we are measuring the rate of virus arriving the epithelium, an essentially 1D process, the actual simulated random walks are in 3D. Ab binding and unbinding to virus were simulated with a Poisson random variable with rates given by eq 1. Lastly, Ab–mucin interactions were simulated with Poisson random variables and rates dependent on the total number of virion-bound Abs and

those Abs currently interacting with mucins. Due to the great computational expense involved in simulating Ab–mucin interactions, particularly when $m_{\text{on}}[M] > m_{\text{off}}$, we computed lookup tables giving the distributions for the time that a virion spends freely diffusing and the time that a virion spends interacting with mucins (see the Supporting Information and Figure S1). The (random) time that a virion spends freely diffusing is given by the last time that none of the surface-bound Abs associate with mucin until the next time that at least one of its associated Abs binds to mucin. Similarly, the time that a virion spends interacting with mucins is given by the last time that at least one of the virion-bound Abs associates with mucin until the next time that none of the surface-bound Abs associate with mucin. We then sampled from these lookup tables whenever a virion's state changes (freely diffusing or bound to mucin, binding or unbinding an Ab, crossing the semen/CVM interface). These methods were used to generate data presented in Figure 2.

The second simulation method consists of a reaction–diffusion PDE to capture the average behavior of the virus population. The virus population is represented by a vector $\vec{V}(z, t)$, where the component $V_n(z, t)$ represents the concentration of virus with n bound Abs. We previously introduced a parameter $\alpha = (m_{\text{off}}/(m_{\text{off}} + [M]m_{\text{on}}))$ to represent the fraction of time that Abs in CVM spend freely diffusing.¹¹ Because Ab–mucin interactions likely occur at fast time scales,

$$u_f(z, t) = \begin{cases} \alpha u(z, t), & 0 < d < 50 \\ u(z, t), & 200 < d < 250 \end{cases}$$

and

$$u_b(z, t) = u(z, t) - u_f(z, t)$$

In the limit $m_{\text{on}}, m_{\text{off}} \rightarrow \infty$ (keeping $m_{\text{off}}/(m_{\text{off}} + [M]m_{\text{on}})$ fixed), the stochastic model can thus be approximated by the reaction–diffusion system

$$\frac{\partial \vec{V}}{\partial t} = D \frac{\partial^2 \vec{V}}{\partial z^2} + \vec{f}(\vec{V}, u) - \vec{g}(\vec{V}, u)$$

$$\frac{\partial u}{\partial t} = D_{\text{Ab0}} \frac{\partial^2 u}{\partial z^2}$$

where the diffusion tensor \mathbf{D} is a diagonal tensor with entries $D_{v0}, \beta_1 D_{v0}, \dots, \beta_{3N_*} D_{v0}$ along the diagonal (the diffusion factors β_i are determined below) for $0 < d < 50$ and diagonal

entries are all D_{v0} for $50 < d < 250$; $D_{\text{Ab}} = \begin{cases} \alpha D_{\text{Ab0}}, & 0 < d < 50 \\ D_{\text{Ab0}}, & 50 < d < 250 \end{cases}$; and the reaction terms

$\vec{f}(\vec{V}, u)$ and $\vec{g}(\vec{V}, u)$ have entries

$$f_n = (3N_* - n + 1)[k_{\text{on}}^f u_f(z, t) + k_{\text{on}}^b u_b(z, t)]V_{n-1}(z, t)\chi_{n>0} + (n+1)k_{\text{off}}V_{n+1}(z, t) - \chi_{n<3N_*} \text{ and}$$

$g_n = (3N_*)[k_{\text{on}}^f u_f(z, t) + k_{\text{on}}^b u_b(z, t)]V_n(z, t) + nk_{\text{off}}V_n(z, t)$ for $n = 0, 1, \dots, 3N_*$, respectively, with χ denoting the indicator function.

Simultaneous Diffusion of HIV and Ab

We use a forward-time central-space scheme to model diffusion for both the virus and Ab populations in 3D, with reflecting boundary conditions at the semen/lumen interface, reflecting conditions for Ab and absorbing conditions for virus at the CVM/cell interface, and Fick's law for the discontinuous diffusion coefficients at the semen/CVM interface. We assume that the number of Abs binding to virions is negligible compared to the overall Ab population, so there are no local depletion effects.

If each virion-bound IgG binds and unbinds to the mucin mesh independently, then the virion spends approximately a fraction α^n of time with all its bound Abs simultaneously free from mucin. This yields a time-averaged diffusivity for the virion of $D_{vn} = \alpha^n D_{v0}$ in CVM. One adjustment is made, however, to account for the lower diffusivity of a virion–Ab complex compared with an individual Ab. Similar to the adjustments on k_{on} , we define $m^{\text{first}} = (1/30)$, so that initial Ab–mucin encounters occur at rate $m^{\text{first}}m_{\text{on}}[\text{M}]$. For subsequent interactions of virion-bound Abs with mucin, the rate may increase because the Ab–virus complex is already located in close proximity to a mucin molecule or may decrease due to the reduced diffusivity of the Ab–virus complex associated with mucins relative to a nonassociated Ab–virus complex. Due to the lack of empirical data in the literature, we assumed other Abs bound to the same virion with at least one Ab already associating with mucins will associate with mucins with the same mucin-binding kinetics as a free Ab molecule. To calculate the diffusion factors $\beta_1, \beta_2, \dots, \beta_{3N_*}$, we first neglect the factor m^{first} and consider the total time free_{*i*} that a virion with *i* bound Abs spends freely diffusing and the total time bound_{*i*} that it spends bound to mucins up to a time *T*. Because the Abs are assumed to bind and unbind to mucin independently, $\lim_{T \rightarrow \infty} (\text{free}_i / (\text{free}_i + \text{bound}_i)) = \alpha^i$, and thus $\beta_i = (\text{free}_i / m^{\text{first}}) / (\text{free}_i / m^{\text{first}} + \text{bound}_i) = \alpha^i / (\alpha^i + m^{\text{first}}(1 - \alpha^i))$.

The stochastic simulations and the reaction–diffusion simulations show excellent agreement, particularly at rapid $m_{\text{on}}[\text{M}]$ and m_{off} . Indeed, for $m_{\text{on}}[\text{M}] = 10^1 \text{ s}^{-1}$, the difference between stochastic simulations and the reaction–diffusion simulations is on average ~8.5% and decreases to an average of ~3.5% for $m_{\text{on}}[\text{M}] = 10^2 \text{ s}^{-1}$ (Figure S3; see the Supporting Information for theoretical estimates of $m_{\text{on}}[\text{M}]$ and m_{off}). Hence, we used the deterministic simulations except where noted. These methods were used to generate data presented in Figures 3A,B, 4A,B, and 5A,B.

Env Neutralization by Binding Abs

In addition to measuring reduction in the flux of viruses arriving at the epithelium, we also incorporated virus infectivity and extent of Ab neutralization in our analysis. Determining the number of Abs required to neutralize a given HIV remains an active area of research, due to the difficulty in simultaneously distinguishing the number of Abs necessary to neutralize a particular Env spike and the minimum number of Ab-free Env spikes necessary for HIV to successfully infect.²⁷ It was previously proposed that the binding of a single Ab molecule to an Env spike appears to be sufficient to inactivate the infectivity associated with

that spike.²⁸ The minimum number of Ab-free Env spikes and, consequently, the number of Env spikes that must be inactivated to neutralize a virion, remain more controversial. Estimates for minimum infectivity range from a single Ab-free Env spike²⁸ to many.²⁹ For our current model, we assume that each additional Ab binding to a previously unoccupied Env incrementally reduces the likelihood of infection, and we measure the overall reduction in infectivity by the reduction in number of unoccupied Env arriving at the vaginal epithelium over the first 2 h post-ejaculation. These methods were used to generate data presented in Figures 3C,D, 4C,D, and 5C,D.

Supplementary Material

Refer to Web version on PubMed Central for supplementary material.

Acknowledgments

Funding

This work was supported by National Institutes of Health (<http://www.nih.gov/>) Grants R21AI093242 (S.K.L.) and U19AI096398 (S.K.L. and R.C.); the National Science Foundation (<http://www.nsf.gov/>) DMS-1122483 (M.G.F.), DMS-1100281 (M.G.F.), and CAREER Award DMR-1151477 (S.K.L.); the Simons Foundation (<https://www.simonsfoundation.org/>) Project 245653 (S.A.M.); the Packard Foundation (<http://www.packard.org/>) (S.K.L.); and startup funds from the Eshelman School of Pharmacy (<https://pharmacy.unc.edu/>) and Lineberger Comprehensive Cancer Center at the University of North Carolina—Chapel Hill (<https://unclineberger.org/>) (S.K.L.). The funders had no role in study design, data collection and analysis, decision to publish, or preparation of the manuscript.

ABBREVIATIONS

Ab	antibody
CVM	cervicovaginal mucus
IgG	immunoglobulin G

REFERENCES

1. (a) Casadevall A, Pirofski LA. A new synthesis for antibody-mediated immunity. *Nat. Immunol.* 2012; 13(1):21–28. [PubMed: 22179281] (b) Corthesy B. Role of secretory immunoglobulin A and secretory component in the protection of mucosal surfaces. *Future Microbiol.* 2010; 5(5):817–829. [PubMed: 20441552] (c) Kozlowski PA, Neutra MR. The role of mucosal immunity in prevention of HIV transmission. *Curr. Mol. Med.* 2003; 3(3):217–228. [PubMed: 12699359]
2. (a) Burton DR, Mascola JR. Antibody responses to envelope glycoproteins in HIV-1 infection. *Nat. Immunol.* 2015; 16(6):571–576. [PubMed: 25988889] (b) van Gils MJ, Sanders RW. Broadly neutralizing antibodies against HIV-1: templates for a vaccine. *Virology.* 2013; 435(1):46–56. [PubMed: 23217615]
3. (a) Dunkelberger JR, Song WC. Complement and its role in innate and adaptive immune responses. *Cell Res.* 2010; 20(1):34–50. [PubMed: 20010915] (b) Huber M, Olson WC, Trkola A. Antibodies for HIV treatment and prevention: window of opportunity? *Curr. Top. Microbiol. Immunol.* 2008; 317:39–66. [PubMed: 17990789] (c) Kilian, M.; Russell, MW. Function of mucosal immunoglobulins. In: Ogra, PL.; Mestecky, J.; Lamm, ME.; Strober, W.; Bienenstock, J.; McGhee, JR., editors. *Handbook of Mucosal Immunology*. San Diego, CA, USA: Academic Press; 1994. p. 127-137.
4. (a) Whaley KJ, Zeitlin L, Barratt RA, Hoen TE, Cone RA. Passive immunization of the vagina protects mice against vaginal transmission of genital herpes infections. *J. Infect. Dis.* 1994; 169(3):

- 647–649. [PubMed: 8158042] (b) Zeitlin L, Whaley KJ, Sanna PP, Moench TR, Bastidas R, De Logu A, Williamson RA, Burton DR, Cone RA. Topically applied human recombinant monoclonal IgG1 antibody and its Fab and F(ab')₂ fragments protect mice from vaginal transmission of HSV-2. *Virology*. 1996; 225(1):213–215. [PubMed: 8918548] (c) Veazey RS, Shattock RJ, Pope M, Kirijan JC, Jones J, Hu Q, Ketas T, Marx PA, Klasse PJ, Burton DR, Moore JP. Prevention of virus transmission to macaque monkeys by a vaginally applied monoclonal antibody to HIV-1 gp120. *Nat. Med.* 2003; 9(3):343–346. [PubMed: 12579198] (d) Mascola JR, Stiegler G, VanCott TC, Katinger H, Carpenter CB, Hanson CE, Beary H, Hayes D, Frankel SS, Birx DL, Lewis MG. Protection of macaques against vaginal transmission of a pathogenic HIV-1/SIV chimeric virus by passive infusion of neutralizing antibodies. *Nat. Med.* 2000; 6(2):207–210. [PubMed: 10655111]
5. (a) Chipperfield EJ, Evans BA. Effect of local infection and oral contraception on immunoglobulin levels in cervical mucus. *Infect. Immun.* 1975; 11(2):215–221. [PubMed: 163217] (b) Usala SJ, Usala FO, Haciski R, Holt JA, Schumacher GF. IgG and IgA content of vaginal fluid during the menstrual cycle. *J. Reprod. Med.* 1989; 34(4):292–294. [PubMed: 2715991] (c) Wang YY, Kannan A, Nunn KL, Murphy MA, Subramani DB, Moench T, Cone R, Lai SK. IgG in cervicovaginal mucus traps HSV and prevents vaginal herpes infections. *Mucosal Immunol.* 2014; 7(5):1036–1044. [PubMed: 24496316]
 6. Lai SK, Wang YY, Hida K, Cone R, Hanes J. Nanoparticles reveal that human cervicovaginal mucus is riddled with pores larger than viruses. *Proc. Natl. Acad. Sci. U. S. A.* 2010; 107(2):598–603. [PubMed: 20018745]
 7. (a) Lai SK, Hida K, Shukair S, Wang YY, Figueiredo A, Cone R, Hope TJ, Hanes J. Human immunodeficiency virus type 1 is trapped by acidic but not by neutralized human cervicovaginal mucus. *J. Virol.* 2009; 83(21):11196–11200. [PubMed: 19692470] (b) Nunn KL, Wang YY, Harit D, Humphrys MS, Ma B, Cone R, Ravel J, Lai SK. Enhanced trapping of HIV-1 by human cervicovaginal mucus is associated with *Lactobacillus crispatus* dominant microbiota. *mBio.* 2015; 6(5):e01084–e01015. [PubMed: 26443453] (c) Shukair SA, Allen SA, Cianci GC, Stieh DJ, Anderson MR, Baig SM, Gioia CJ, Sponberg EJ, Kauffman SM, McRaven MD, Lakounga HY, Hammond C, Kiser PF, Hope TJ. Human cervicovaginal mucus contains an activity that hinders HIV-1 movement. *Mucosal Immunol.* 2013; 6(2):427–434. [PubMed: 22990624]
 8. (a) Saltzman WM, Radomsky ML, Whaley KJ, Cone RA. Antibody diffusion in human cervical mucus. *Biophys. J.* 1994; 66(2 Part 1):508–515. [PubMed: 8161703] (b) Olmsted SS, Padgett JL, Yudin AI, Whaley KJ, Moench TR, Cone RA. Diffusion of macromolecules and virus-like particles in human cervical mucus. *Biophys. J.* 2001; 81(4):1930–1937. [PubMed: 11566767]
 9. McKinley SA, Chen A, Shi F, Wang S, Mucha PJ, Forest MG, Lai SK. Modeling neutralization kinetics of HIV by broadly neutralizing monoclonal antibodies in genital secretions coating the cervicovaginal mucosa. *PLoS One.* 2014; 9(6):e100598. [PubMed: 24967706]
 10. (a) Klein F, Mouquet H, Dosenovic P, Scheid JF, Scharf L, Nussenzweig MC. Antibodies in HIV-1 vaccine development and therapy. *Science.* 2013; 341(6151):1199–1204. [PubMed: 24031012] (b) Whaley KJ, Mayer KH. Strategies for preventing mucosal cell-associated HIV transmission. *J. Infect. Dis.* 2014; 210(Suppl. 3):S674–S680. [PubMed: 25414423]
 11. Chen A, McKinley SA, Wang S, Shi F, Mucha PJ, Forest MG, Lai SK. Transient antibody-mucin interactions produce a dynamic molecular shield against viral invasion. *Biophys. J.* 2014; 106(9):2028–2036. [PubMed: 24806935]
 12. Smoluchowski, Mv. Versuch einer mathematischen Theorie der Koagulationskinetik kolloider Lösungen. *Z. Phys. Chem.* 1917; 92:129–168.
 13. Sherwood JK, Zeitlin L, Whaley KJ, Cone RA, Saltzman M. Controlled release of antibodies for long-term topical passive immunoprotection of female mice against genital herpes. *Nat. Biotechnol.* 1996; 14(4):468–471. [PubMed: 9630921]
 14. (a) Ramessar K, Rademacher T, Sack M, Stadlmann J, Platis D, Stiegler G, Labrou N, Altmann F, Ma J, Stoger E, Capell T, Christou P. Cost-effective production of a vaginal protein microbicide to prevent HIV transmission. *Proc. Natl. Acad. Sci. U. S. A.* 2008; 105(10):3727–3732. [PubMed: 18316741] (b) Whaley KJ, Hiatt A, Zeitlin L. Emerging antibody products and *Nicotiana* manufacturing. *Hum. Vaccines.* 2011; 7(3):349–356.
 15. (a) Liu HF, Ma J, Winter C, Bayer R. Recovery and purification process development for monoclonal antibody production. *mAbs.* 2010; 2(5):480–499. [PubMed: 20647768] (b) Zydney

AL. Continuous downstream processing for high value biological products - a review. *Biotechnol. Bioeng.* 2015;25695.

16. Santra S, Tomaras GD, Warrier R, Nicely NI, Liao HX, Pollara J, Liu P, Alam SM, Zhang R, Cocklin SL, Shen X, Duffy R, Xia SM, Schutte RJ, Pemble Iv CW, Dennison SM, Li H, Chao A, Vidnovic K, Evans A, Klein K, Kumar A, Robinson J, Landucci G, Forthal DN, Montefiori DC, Kaewkungwal J, Nitayaphan S, Pitisuttithum P, Rerks-Ngarm S, Robb ML, Michael NL, Kim JH, Soderberg KA, Giorgi EE, Blair L, Korber BT, Moog C, Shattock RJ, Letvin NL, Schmitz JE, Moody MA, Gao F, Ferrari G, Shaw GM, Haynes BF. Human non-neutralizing HIV-1 envelope monoclonal antibodies limit the number of founder viruses during SHIV mucosal infection in rhesus macaques. *PLoS Pathog.* 2015; 11(8):e1005042. [PubMed: 26237403]
17. Rerks-Ngarm S, Pitisuttithum P, Nitayaphan S, Kaewkungwal J, Chiu J, Paris R, Prensri N, Namwat C, de Souza M, Adams E, Benenson M, Gurunathan S, Tartaglia J, McNeil JG, Francis DP, Stablein D, Birx DL, Chunsuttiwat S, Khamboonruang C, Thongcharoen P, Robb ML, Michael NL, Kunasol P, Kim JH. Vaccination with ALVAC and AIDSVAX to prevent HIV-1 infection in Thailand. *N. Engl. J. Med.* 2009; 361(23):2209–2220. [PubMed: 19843557]
18. (a) Jamison PL, Gebhard PH. Penis size increase between flaccid and erect states: an analysis of the Kinsey data. *J. Sex Res.* 1988; 24(1):177–183. [PubMed: 22375645] (b) Pendergrass PB, Belovicz MW, Reeves CA. Surface area of the human vagina as measured from vinyl polysiloxane casts. *Gynecol. Obstet. Invest.* 2003; 55(2):110–113. [PubMed: 12771458]
19. Lai SK, O'Hanlon DE, Harrold S, Man ST, Wang YY, Cone R, Hanes J. Rapid transport of large polymeric nanoparticles in fresh undiluted human mucus. *Proc. Natl. Acad. Sci. U. S. A.* 2007; 104(5):1482–1487. [PubMed: 17244708]
20. (a) Geonnotti AR, Katz DF. Dynamics of HIV neutralization by a microbicide formulation layer: biophysical fundamentals and transport theory. *Biophys. J.* 2006; 91(6):2121–2130. [PubMed: 16815899] (b) Lai BE, Henderson MH, Peters JJ, Walmer DK, Katz DF. Transport theory for HIV diffusion through in vivo distributions of topical microbicide gels. *Biophys. J.* 2009; 97(9):2379–2387. [PubMed: 19883580]
21. Gupta P, Mellors J, Kingsley L, Riddler S, Singh MK, Schreiber S, Cronin M, Rinaldo CR. High viral load in semen of human immunodeficiency virus type 1-infected men at all stages of disease and its reduction by therapy with protease and nonnucleoside reverse transcriptase inhibitors. *J. Virol.* 1997; 71(8):6271–6275. [PubMed: 9223532]
22. Rehan N, Sobrero AJ, Fertig JW. The semen of fertile men: statistical analysis of 1300 men. *Fertil. Steril.* 1975; 26(6):492–502. [PubMed: 1169171]
23. Scheid JF, Mouquet H, Ueberheide B, Diskin R, Klein F, Oliveira TY, Pietzsch J, Fenyo D, Abadir A, Velinon K, Hurley A, Myung S, Boulad F, Poignard P, Burton DR, Pereyra F, Ho DD, Walker BD, Seaman MS, Bjorkman PJ, Chait BT, Nussenzweig MC. Sequence and structural convergence of broad and potent HIV antibodies that mimic CD4 binding. *Science.* 2011; 333(6049):1633–1637. [PubMed: 21764753]
24. Zhu P, Liu J, Bess J Jr, Chertova E, Lifson JD, Grise H, Ofek GA, Taylor KA, Roux KH. Distribution and three-dimensional structure of AIDS virus envelope spikes. *Nature.* 2006; 441(7095):847–852. [PubMed: 16728975]
25. (a) Stone A, Gamble CJ. The quantity of vaginal fluid. *Am. J. Obstet. Gynecol.* 1959; 78(2):279–281. [PubMed: 13670196] (b) Owen DH, Katz DF. A vaginal fluid simulant. *Contraception.* 1999; 59(2):91–95. [PubMed: 10361623]
26. Chakraborty H, Sen PK, Helms RW, Vernazza PL, Fiscus SA, Eron JJ, Patterson BK, Coombs RW, Krieger JN, Cohen MS. Viral burden in genital secretions determines male-to-female sexual transmission of HIV-1: a probabilistic empiric model. *AIDS.* 2001; 15(5):621–627. [PubMed: 11317000]
27. Magnus C, Regoes RR. Estimating the stoichiometry of HIV neutralization. *PLoS Comput. Biol.* 2010; 6(3):e1000713. [PubMed: 20333245]
28. Yang X, Kurteva S, Lee S, Sodroski J. Stoichiometry of antibody neutralization of human immunodeficiency virus type 1. *J. Virol.* 2005; 79(6):3500–3508. [PubMed: 15731244]
29. (a) Schonning K, Lund O, Lund OS, Hansen JE. Stoichiometry of monoclonal antibody neutralization of T-cell line-adapted human immunodeficiency virus type 1. *J. Virol.* 1999; 73(10):8364–8370. [PubMed: 10482587] (b) McLain L, Dimmock NJ. Single- and multi-hit kinetics of

immunoglobulin G neutralization of human immunodeficiency virus type 1 by monoclonal antibodies. J. Gen. Virol. 1994; 75(Part 6):1457–1460. [PubMed: 8207410]

Author Manuscript

Author Manuscript

Author Manuscript

Author Manuscript

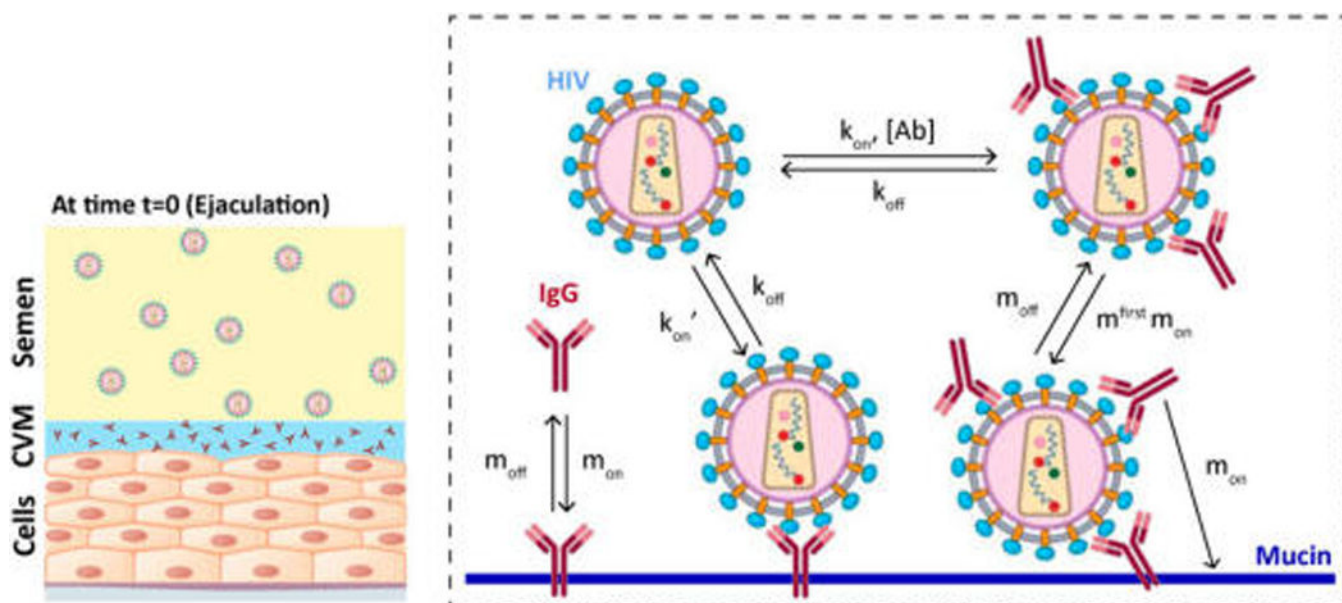


Figure 1.

Schematic of our model that captures the dynamics of HIV from seminal fluid diffusing across a cervicovaginal mucus (CVM) layer containing HIV-binding IgG to reach the underlying vaginal epithelium. To reduce infection, IgG must bind to HIV in sufficient quantities to neutralize or to trap the virions in mucus before HIV virions successfully penetrate CVM. Our model captures the tandem effects of IgG–antigen binding kinetics (k_{on} , k_{off}) as well as IgG–mucin interactions (m_{on} , m_{off}).

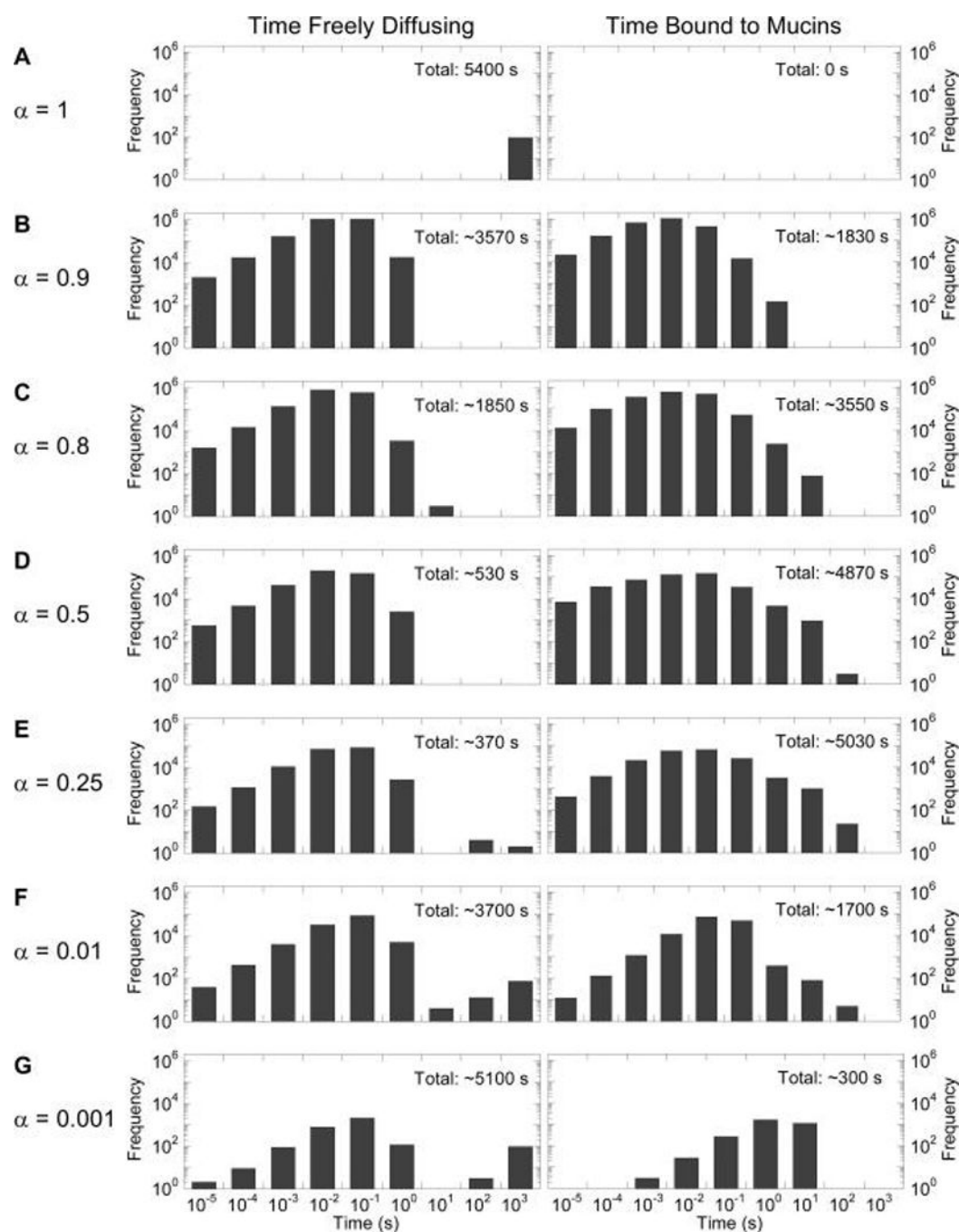


Figure 2.

Distribution of time HIV virions spend freely diffusing or associated with mucins in CVM containing 1 µg/mL NIH45-46 with different affinity to mucins, ranging from no affinity at $\alpha = 1$ to very strong affinity at $\alpha = 0.001$. To minimize bias toward virions with no surface-bound IgG undergoing free diffusion, Abs are allowed to accumulate on HIV for 30 min first prior to measuring the time of free diffusion or association with mucins for the subsequent 90 min.

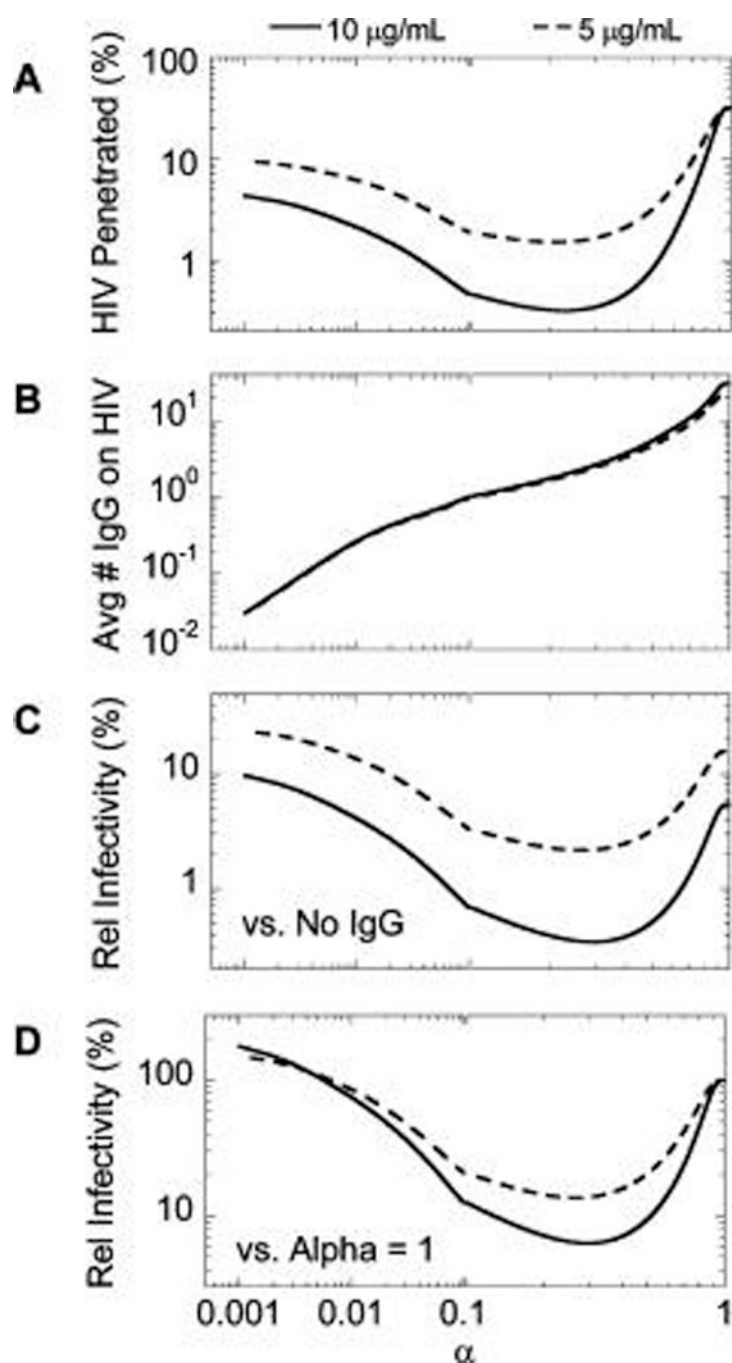


Figure 3.

Predicted trapping potency and protection by 5 and 10 µg/mL NIH45-46 with varying affinity to mucins as characterized by α : (A) predicted fraction of HIV load initially in semen that can diffuse across CVM containing NIH45-46 over the first 2 h post-deposition; (B) average number of NIH45-46 bound to HIV arriving at the vaginal epithelium (values <1 represent HIV virions that arrive at the vaginal epithelium without any bound NIH45-46); (C, D) extent of NIH45-46-mediated protection, as quantified by infectivity

relative to (C) no NIH45-46 present in CVM or (D) the same amount of NIH45-46 present but without any affinity to mucins.

Author Manuscript

Author Manuscript

Author Manuscript

Author Manuscript

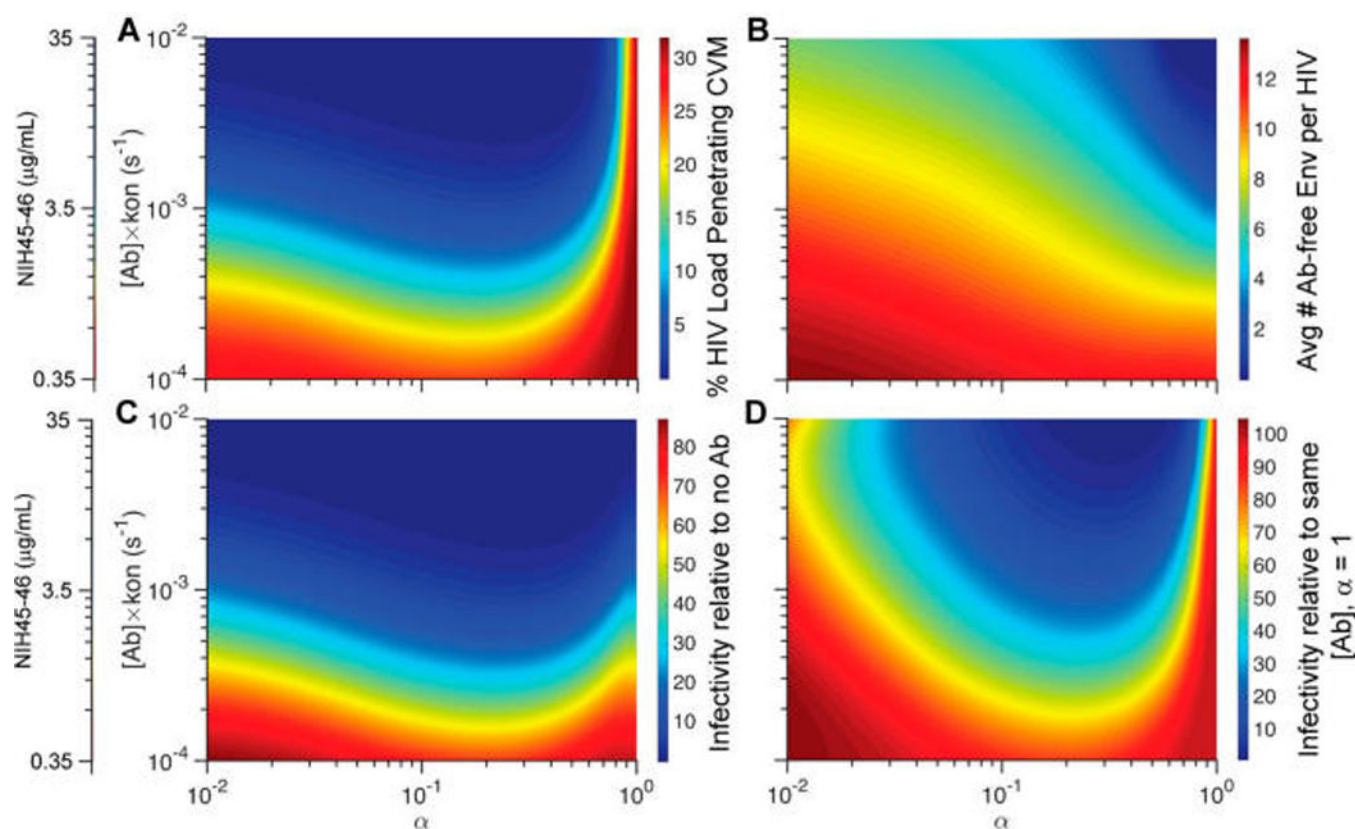


Figure 4.

Phase diagrams mapping the predicted trapping potency and protection as a function of NIH45-46 concentration in CVM and IgG affinity to mucins as characterized by α : (A) fraction of HIV load initially in semen that can diffuse across CVM containing NIH45-46 over the first 2 h post-deposition; (B) average number of Ab-free Env trimers on HIV arriving at the vaginal epithelium; (C, D) extent of NIH45-46-mediated protection, as quantified by infectivity relative to (C) no NIH45-46 present in CVM or (D) the same amount of NIH45-46 present but without any affinity to mucins.

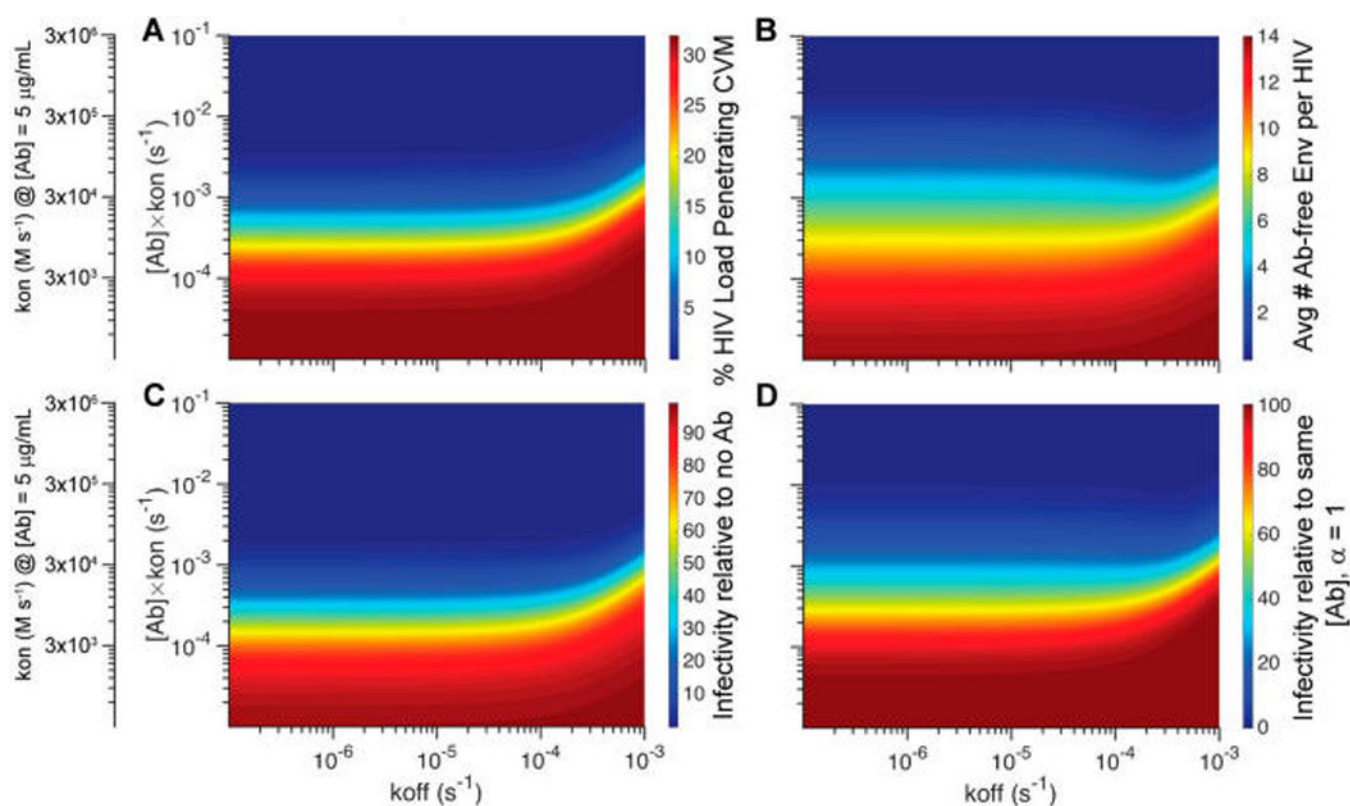


Figure 5.

Phase diagrams mapping the predicted trapping potency and protection as a function of NIH45-46 unbinding kinetics from HIV virions (k_{off}) as well as accumulation kinetics on HIV virions, which is influenced by both the local NIH45-46 concentrations and the binding rate (k_{on}): (A) fraction of HIV load initially in semen that can diffuse across CVM containing NIH45-46 over the first 2 h post-deposition; (B) average number of Ab-free Env trimers on HIV arriving at the vaginal epithelium; (C, D) extent of NIH45-46-mediated protection, as quantified by infectivity relative to (C) no NIH45-46 present in CVM or (D) the same amount of NIH45-46 present but without any affinity to mucins.

Table 1

Parameters and Values Incorporated into the Model

parameter	symbol	value	refs
HIV-1			
diffusivity in CVM	D_v	$1.27 \mu\text{m}^2/\text{s}^a$	7a
diffusivity in semen		assume same as in CVM	
viral load in semen		8.4×10^5 copies/ejaculate ^b	21, 22
no. of Env trimer spikes	N_s	14 ± 7 (SD)	24
IgG			
diffusivity in CVM	D_{Ab}	$40 \mu\text{m}^2/\text{s}$	8
diffusivity in semen		assume same as in CVM	
IgG concentration in CVM		variable	
IgG–Env affinity	k_{on}, k_{off}	variable	
IgG–mucin affinity	$m_{on} [M], m_{off}$	variable	
ratio of D_{Ab} vs diffusivity in buffer	α	variable	
vagina			
surface area of lumen	SA_{vagina}	145 cm^2^c	18a,b
volume of luminal CVM	V_{CVM}	$\sim 750 \mu\text{L}$	25
thickness of CVM layer	L	$50 \mu\text{m}^d$	
volume of semen	V_{semen}	$\sim 3.0 \text{ mL}$	22
thickness of semen layer	d	$200 \mu\text{m}^d$	

^aThe geometrically averaged D_{eff} for HIV was previously measured to be $0.25 \mu\text{m}^2/\text{s}$, but with a substantial fraction of viruses exhibiting more rapid mobility. For the current analysis, we used $1.27 \mu\text{m}^2/\text{s}$, which represents the top 25th percentile of virus mobility; this is in reasonable agreement with a more recent study of HIV diffusion in genital secretions.^{7c}

^bEstimated on the basis of a median semen volume of 3.0 mL^{22} and 2.8×10^5 HIV-1 RNA copies/mL, which represents the upper limit of HIV-1 RNA copies/mL in seminal plasma from ref 21. This is in reasonable agreement with another report by Chakraborty et al., which estimated 5×10^5 HIV-1 RNA copies/ejaculate, with a maximum of about 2×10^7 HIV-1 RNA copies/ejaculate.²⁶

^cThe mean surface area of the vagina in the native state was previously estimated to be $\sim 90 \text{ cm}^2$ by injection of vinyl polysiloxane casts vaginally. Alternatively, the surface area of vaginal lumen may also be inferred by the surface area of the erect penis (average $\sim 200 \text{ cm}^2$) assuming complete insertion into the vagina. We took the average from the two approaches.

^dCVM (L) and semen (d) thicknesses are estimated by $V_{\text{CVM}}/SA_{\text{vagina}}$ and $V_{\text{semen}}/SA_{\text{vagina}}$, respectively.